DOA Estimation in Wireless Seismic Surveys Using Deep Learning

A. Almehdhar, A. Hamida, K. Aliyu, S. Alawsh, A. Muqaibel, S. Al-Dharrab, W. Mesbah
Electrical Engineering Department
King Fahd University of Petroleum & Minerals
Dhahran 31261, Saudi Arabia
{g201472900, g201425140, g201705110, salawsh, muqaibel, suhaild, mesbahw}@kfupm.edu.sa

Gordon L. Stüber
School of Electrical and Computer Engineering
Georgia Institute of Technology
Atlanta, GA 30332, USA
stuber@ece.gatech.edu

***Abstract*— Current seismic survey systems use wired telemetry to collect seismic data from sensors (geophones), and due to the massive cabling requirement, the current wired systems are limited by weight and cost. Replacing current systems with wireless technologies is becoming a more practical and economical choice. Once sensors are wireless, localizing them becomes a necessity when interpreting seismic data. Direction of Arrival (DOA) estimation can be used for source localization. In this paper, DOA estimation based on Deep Neural Network (DNN) is proposed for wireless seismic survey. In terms of accuracy in estimation, simulation results are promising.**

Keywords—Deep Neural Network; Direction of Arrival; Geophone; Wireless Seismic Surveys.

I. INTRODUCTION

Currently, oil and gas are the main sources of energy. Due to their importance, substantial research is directed to improve methods for exploring reservoirs of these natural resources. One of the common exploration methods is the seismic survey. Seismic data acquisition or seismic surveying is a process in which the underground structure is investigated [1]. The process uses a source to create vibrations on the ground which generate acoustic signals that propagate through the crust of the earth and experience different reflections from different layers of the crust. The reflected signals travel back to the ground and are detected by sensors. These sensors could be either geophones or accelerometers. A geophone is a ground-motion transducer that converts the ground movements into voltage. Current seismic survey systems mostly use wired geophones, which for large scale surveys can result in a huge amount of cables that can be up to hundreds of kilometers. This massive cabling requirement introduces constraints and inflexibility on the survey geometry design [2]. In addition, cables can form up to 50% of the total survey cost and up to 75% of total survey equipment weight [3]. Consequently, this leads to inefficiencies and high transportation costs, which can be avoided if wireless technologies are incorporated in seismic surveys. Wireless systems often use knowledge about the Direction of Arrival (DOA) of the signal. Generally, DOA can be used to locate a source or to enable the antenna to form a beam in the direction of the signal to enhance the transmission and reception efficiency.

Wireless seismic surveys are yet to be fully incorporated in the field. However, in the literature, there are some proposed wireless communication models. In general, the models represent a large network of geophones managed by nodes that transmit the geophones readings to a central office. In [4], Tian adopted a wireless sensor system following a star topology, where multiple geophones are connected to a single gateway node. The geophones send the seismic data continuously, and the gateways capture the data every fixed time-period and send it to the central office. In [5], Savazzi *et al*. proposed a system that handles a large number of geophones in the range of $20{,}000 - 30{,}000$ that are simultaneously active with a typical land distribution density of 2000 geophone/sqkm. The authors divided the geometric model into sub-networks, where each sub-network contains a single gateway node coordinating 300 geophones. The authors in [3] and [6] modified the network by clustering geophones to transmit seismic data to a cluster-head node, which is an intermediate node that passes the data from several geophones to the gateway. In [7], an orthogonal geometry for a typical geophone network is described, where the Receiver Lines (RLs) and the Source Lines (SLs) are perpendicular to each other. Geophones are distributed along the RLs with separation of $5 - 30\ m$, and vibration sources take shots along the SLs. A total of 30 RLs are assumed to cover an area of $72\ km^2$, and each RL consists of 480 geophones summing up to a total of 14400 geophones.

Regarding the used communication technologies, Savazzi *et al*. compared different communication technologies for short-range communication, which is done inside the sub-network, such as ZigBee, Bluetooth, Impulse Radio Ultra-Wide Band (IR-UWB), Multi Band-Orthogonal Frequency Division Multiplexing (MB-OFDM), and Wi-Fi [2]. Also, candidates for long range communication technology to be used between sub-networks and the central office were compared; these includes cellular systems (EDGE and UMTS), Wi-Fi, and WiMAX. In [3] and [6], Savazzi *et al*. proposed using IR-UWB for short-range communications due to its support for high data rates. In addition, it is noted that Wi-Fi is a good candidate for long-range communications but lacks energy efficiency. In [7], power saving geophone network protocols are described that are compliant with IEEE $802.11af$ or SuperWiFi which operates in Television White Space (TVWS) frequency bands that range from $50 -$

This work is supported by the Center for Energy and GeoProcessing (CeGP) at Georgia Institute of Technology and King Fahd University of Petroleum and Minerals (KFUPM), under grant number GTEC1601.

978-1-7281-6535-6/20/$31.00 ©2020 IEEE

700 MHz. This is considered to be a large bandwidth that supports huge data rates that are usually required in seismic surveys, with the assumption that seismic surveys are conducted on areas where these frequencies are not utilized.

Many algorithms for DOA estimation have been proposed, such as, Beamforming, Capon, Multiple Signal Classification (MUSIC), Estimation of Signal Parameters via Rotation Invariance Technique (ESPRIT) [8] and recently Deep Learning. Deep learning or Deep Neural Network (DNN) is a multilayer interconnected neural network that received a lot of attention as a result of wide application and high resolution in executing tasks. Some of the applications of DNN includes medicine, radar, sonar, and mobile communications. There have been new attempts to incorporate deep learning in DOA estimation. In [9], the authors used a DNN for finding the DOA of an Unmanned Aerial Vehicle (UAV). Kase *et al* in [10] designed a DNN for a specific two-target DOA estimation scenario and got relatively high accuracy (1° resolution). Zhang *et al* in [11] used DNN for DOA in 1° resolution. Moreover, Lui-li *et al* in [12] used deep convolution for DOA estimation in approximating real-time response. On the other hand, Huang *et al* in [13] used deep learning for super-resolution DOA estimation based on a massive Multiple-Input Multiple-Output (MIMO) system, which is a close match to the application in hand since the seismic survey system may be modeled as a massive MIMO system for large scale seismic surveys.

In this paper, different DNNs with various network structures are evaluated for DOA estimation. One network structure is chosen based on its performance on multiple criteria. The chosen network is applied in a simulated seismic survey to estimate the DOA of wireless geophone at cluster-head node. The remainder of this paper is organized as follows. In Section II, the system model is presented including the seismic geometric model, the MIMO model and the deep learning model. Simulation and results are provided in Section III, which is followed by a conclusion in Section IV.

Notations: In this paper vectors are represented by boldface small letters, whereas matrices are denoted by boldface capital letters. Transpose and Hermitian operators are represented by $[\cdot]^T$ and $[\cdot]^H$, respectively. The symbols $\Re(\cdot)$ and $\Im(\cdot)$ represent the real and imaginary parts of their inputs, respectively.

II. System Model

A. Nodes Distribution Model

In this paper, we adopted a three-level geometry in which the system consists of geophones, cluster-head nodes and gateways. The process of wireless seismic survey starts by deploying the equipment in a specific manner. The geometry of deployment is described in this section. Once the equipment is deployed, a source of vibration is set on the ground near to the geophones. These vibrations result in acoustic signals propagating through the layers of the crust. The reflected signals penetrate back towards the surface of the earth and are then sensed by geophones. Geophones then digitize and amplify the reflected waves and send these digitized signals to a nearby cluster-head that transmits the data into the nearest gateway node, which, in turn, forwards it to the central office for further processing.

A total number of 99 gateways were assumed in an area of $1\ km \times 10\ km = 10\ km^2$ and are uniformly distributed in lines with a separation of 300 m in both the horizontal and vertical dimensions. Each gateway manages 18 cluster-head nodes. Cluster-head nodes are assumed to have a uniform distribution in lines with a separation of 100 m and 50 m in the horizontal and vertical dimensions, respectively. Each cluster-head node is designed to communicate with 12 to 15 geophones. The geophones are assumed to be randomly distributed in the same lines as cluster-head nodes and have a uniformly distributed random separation in the range of $5 - 30\ m$ in both dimensions. A small section of the geometric model is shown in Fig. 1. Wireless connection can be provided throughout the entire area by dividing the area into hexagonal cells, where each cell is controlled by a cluster-head node.

In order to estimate DOA of received signal, we assume that we have a 120° coverage for each antenna, thus, sectoring the cells is mandatory. Therefore, each cell is divided into three sectors. Zooming into one cell, Fig. 2, shows the three sectors with different set of geophones inside each sector.

Each sector will have its own ULA, tripling the total number of served geophones in each cell. Now, each cluster-head contains three ULAs and communicates with around 45 geophones.

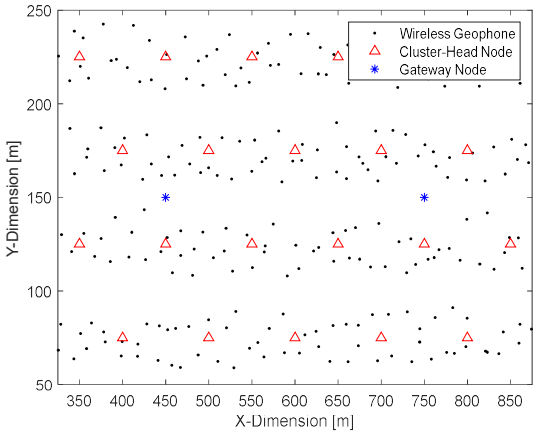

Fig. 1. Geometric model for wireless seismic surveys

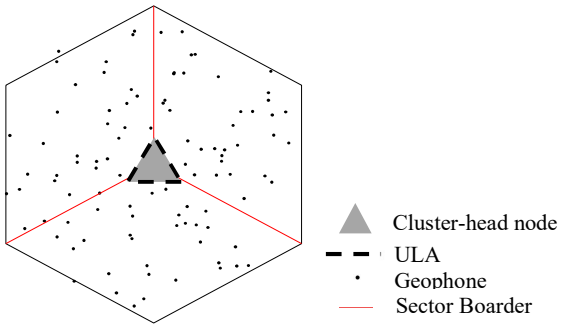

Fig. 2. One cell sensor geometry

B. DOA Estimation Model

As mentioned in previous section II-A, we assume ULA with $d = \lambda/2$ as the spacing between antenna elements, and λ is the wavelength of the transmitted signal, as shown in Fig. 3. It is also assumed that the signal is transmitted far enough from the receiver so that the far-field model is suitably adopted.

We consider a wireless seismic model as a typical MIMO Up-Link system of a Base Station (BS) with N_t-element ULA and K single antenna users. For transmitted signal vector, $\mathbf{x}$, and a channel response, $\mathbf{H}$, we can model the received signal, $\mathbf{y}$, by:

$$\mathbf{y}(t) = \mathbf{H}\mathbf{x}(t) + \mathbf{n}(t) \tag{1}$$

where $\mathbf{n} \sim \mathcal{CN}(0, \sigma^2\mathbf{I}_K)$ is Additive White Gaussian Noise (AWGN), and $\mathbf{H} = [\mathbf{h}_1, \mathbf{h}_2, \dots, \mathbf{h}_K]$, where $\mathbf{h}_k$ is a channel response given as:

$$\mathbf{h}_k = \sum_{i=1}^{P} g_{k,i}\mathbf{a}_t(\theta_{k,i}) = \mathbf{A}_{t,k}\mathbf{g}_k \tag{2}$$

where P represents the number of resolvable paths from the BS to the k^{th} user, $\mathbf{g}_k$ denotes the complex gain of the channel, and $\theta_{k,i}$ represents the physical DOA of the i^{th} path at the k^{th} user. Also, the steering vector $\mathbf{a}_t(\theta_{k,i})$ is defined as the array response of the i^{th} path at the BS. For a ULA, $\mathbf{a}_t(\theta_{k,i})$ can be expressed as [13]:

$$\mathbf{a}_t(\theta_{k,i}) = \frac{1}{\sqrt{N_t}}\left[1, e^{-j2\pi\frac{d}{\lambda}\sin\theta_{k,i}}, \dots, e^{-j2\pi\frac{d}{\lambda}(N_t-1)\sin\theta_{k,i}}\right]^T \tag{3}$$

The steering matrix can be assembled as $\mathbf{A}_{t,k} = \left[\mathbf{a}_t(\theta_{k,1}), \mathbf{a}_t(\theta_{k,2}), \dots, \mathbf{a}_t(\theta_{k,P})\right]$.

Assuming, for simplicity, that the channel can be modeled by the steering vector only without the complex gain, and there is no multipath, the received signal can be written as:

$$\mathbf{y}(t) = \mathbf{A}\mathbf{x}(t) + \mathbf{n}(t) \tag{4}$$

where $\mathbf{A} = [\mathbf{a}(\theta_1), \mathbf{a}(\theta_2), \dots, \mathbf{a}(\theta_K)]$ is the steering matrix.

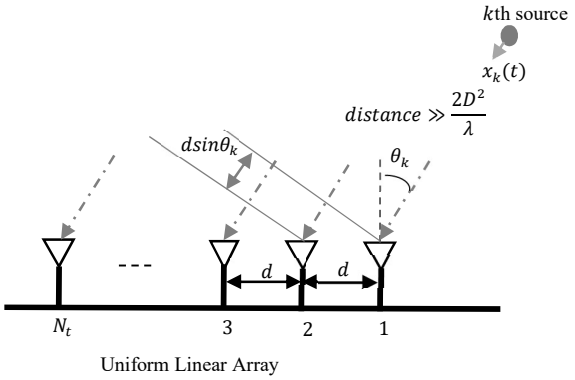

Fig. 3. DOA estimation using ULA

Most DOA estimation algorithms require finding the covariance matrix of the received signal, $\mathbf{R}_{\mathbf{yy}}$, which is given by:

$$\mathbf{R}_{\mathbf{yy}} = E[\mathbf{y}(t)\mathbf{y}^H(t)] = \mathbf{A}\mathbf{R}_{\mathbf{xx}}\mathbf{A}^H + \sigma^2\mathbf{I}_{N_t} \tag{5}$$

where $\mathbf{R}_{\mathbf{xx}} = \mathrm{E}[\mathbf{x}(t)\mathbf{x}^H(t)]$ is the covariance matrix of the transmitted signal and σ^2 is the variance of the noise. In fact, it is not easy to find the exact covariance matrix, thus $\mathbf{R}_{\mathbf{yy}}$ can be estimated over T samples as follows:

$$\mathbf{R}_{\mathbf{yy}} \approx \widehat{\mathbf{R}}_{\mathbf{yy}} = \frac{1}{T}\sum_{i=1}^{T}\mathbf{y}(t_i)\mathbf{y}^H(t_i) = \frac{1}{T}\mathbf{Y}\mathbf{Y}^H \tag{6}$$

where $\mathbf{Y} = [\mathbf{y}(t_1), \mathbf{y}(t_2), \dots, \mathbf{y}(t_T)]^T$.

C. Deep Neural Network Formulation

Recently, the term "deep learning" has been intensively used in many aspects including the DOA estimation, as presented in Section I. The simplest linear one-layer neural network with M inputs can be expressed as:

$$z_j = f(\mathbf{v}, \mathbf{w}) = \sum_{i=1}^{M} v_i w_{j,i} + b_j \tag{7}$$

where $f(\cdot)$, z_j, $\mathbf{v}$, $\mathbf{w}$ and b_j are the output of the layer, input to the layer, weights of the neural network layer and the bias, respectively. Fig. 4 illustrates the layout of the adopted DNN. The adopted deep learning algorithm solves the problem of DOA estimation through a mapping function to generate a weight that has minimum error between any input and the desired output. To estimate DOA, the covariance matrix $\mathbf{R}_{\mathbf{yy}}$ is used as the input to the DNN, denoted by $\boldsymbol{v} = [v_1, v_2, \dots, v_M]$. Since $\mathbf{R}_{\mathbf{yy}}$ is a Hermitian matrix, it is enough to consider its upper or lower triangular entries. In this model, the lower triangular entries of $\mathbf{R}_{\mathbf{yy}}$ is decomposed to the single vector $\boldsymbol{v}$ by taking the diagonal elements first and then all elements below it as one row at a time, and separating the real component from the imaginary one so that the input vector of the DNN is:

$$\boldsymbol{v} = [r_{1,1}, r_{2,2}, \dots, r_{N_t,N_t}, \Re(r_{2,1}), \Im(r_{2,1}), \Re(r_{3,1}), \Im(r_{3,1}), \Re(r_{3,2}), \dots, \Im(r_{N_t,N_t-1})] \tag{8}$$

The output of the input layer is then fed to a multiple hidden layers for feature extraction. Finally, a linear output layer is required to produce the estimated output. The output angles is in the range $-60°$ to $60°$ with 1^o resolution. In this paper, feed-forward neural network with supervised learning technique is used, where the learning algorithm used is Levenberg Marquardt [14]. Moreover, three network parameters are varied to find the optimum performance, which are based on training data in terms of the Signal-to-Noise Ratio (SNR) variation, number of hidden layers and number of neurons in each layer. The following section analyzes the performance of the proposed DNN.

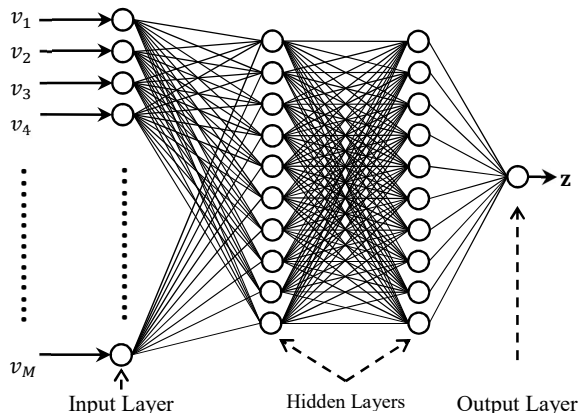

Fig. 4. Structural layout of DNN

III. Simulation And Results

In this section, the performance of the presented algorithm is evaluated using different number of layers and number of neurons in each layer. In Section III-B, the best parameters for the DNN are used in the developed seismic model. We assume single active source at a time, $K = 1$ with randomly generated narrow band signal with carrier frequency of $2.4\,GHz$ at different levels of SNR. The transmitted signal arrive at the ULA of 5-element ULA with DOA in the range from $-60°$ to $60°$ with 1^o resolution which results in 121 possible angles. A total of 300 snapshots (T) is adopted for evaluating the covariance matrix. The number of inputs to DNN is N_t^2 which is 25 for the selected ULA. In the adopted neural network, sigmoid activation function is used in each hidden layer and linear output activation function. The learning algorithm used is Levenberg Marquardt backpropagation and Gradient descent with momentum as adaption function. To avoid overfitting in the network while training, 80 percent of the generated data is used for training the network while the remaining 20 percent is used for validation.

Two performance metrics namely the Root Mean Square Error (RMSE) and the probability of obtaining true DOAs are presented. The RMSE is defined as follows:

$$\text{RMSE} = \sqrt{\frac{1}{KN}\sum_{k=1}^{K}\sum_{n=1}^{N}\left(\hat{\theta}_k^{(n)} - \theta_k^{(n)}\right)^2} \qquad (9)$$

where N and K are the number of tests, N is the number of tests per user, K is the number of users. $\hat{\theta}_k^{(n)}$, and $\theta_k^{(n)}$ are the estimated DOA and actual DOA at the n^{th} test for the k^{th} user. For both metrics, the estimated DOAs are said to be correct whenever their deviation from the actual DOA is within 0.5°.

In order to study the effect of certain types of training data on the performance of the network, we fixed the other two parameters, 2 layers each contains 10 neurons, and we trained the network with four different data sets. These training data sets are generated with varying SNR as follows:

- Constant 0 dB SNR
- Constant 30 dB SNR
- Increasing SNR from 0 dB to 30 dB with steps of 1 dB
- Increasing SNR from 0 dB to 30 dB with steps of 5 dB

There is a total of 6050 data samples per SNR, resulting in a total number of 6050, 6050, 187550 and 42350 data samples for the four mentioned cases, respectively. The four trained neural networks are tested with another data set that contains all 121 angles in all values of integer SNRs from 0 dB to 30 dB. Fig. 5 and Fig. 6 compare the effect of these four training cases on the RMSE and the probability of obtaining correct DOA's, respectively. It is evident from Fig. 5 and Fig. 6 that networks trained with hybrid data (with multiple SNRs) perform much better than those of a single and fixed SNR. Moreover, the network trained with data that contains all 31 different SNRs (1 dB steps) performs slightly better than that of 7 different SNRs (5 dB steps). Training set of hybrid data with 1 dB step is used in the remaining results.

To study the effect of varying the number of neurons in each layer in the network, we fixed the type of training set and the number of layers to be 2. The networks are trained with the same training data set using 10, 30 and 50 neurons and also tested with another unknown data set. Fig. 7 and Fig. 8 present the performance evaluation measures.

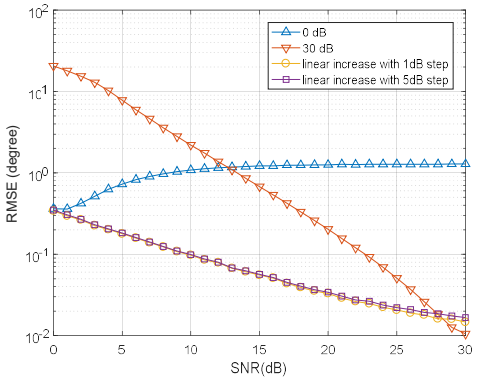

Fig. 5. RMSE for different training conditions

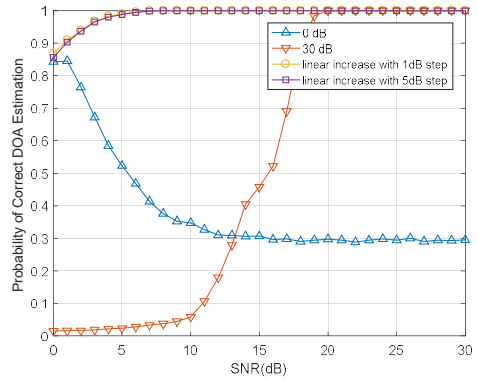

Fig. 6. Probability of correct DOA estimation for different trainings

The RMSE values show comparable performance for all three cases with a slight lead for the case of 30 neurons. Nevertheless, the probability of correct estimation, presented in Fig. 8, also shows comparable performance with a slight lead for the case of 10 neurons. Hence, 10 neurons per layer are adopted.

Finally, the effect of the number of hidden layers in the network is examined, these networks are constructed with up to four hidden layers. All layers in all cases consist of 10 neurons. In addition, all four networks are trained with a common training data set and are tested using another unknown data set. Fig. 9 and Fig. 10 present the performance evaluation measures. Both, the RMSE and the probability of correct estimation, show that among the four tested cases, using 3 hidden layers gives the best results.

Now that we have chosen the best network structure, which uses 3 hidden layers and 10 neurons per layers and is trained by hybrid data with 1 dB step, the transmitted signals from geophones in one sector were simulated to be received by their cluster-head. We inputted these signals to the chosen neural network. and calculated performance measures for this scenario. Results show that out of 18 different DOA of geophone signals, 17 of them were obtained with a resolution of one degree. This gives a probability of correct estimation of 94.44% also RMSE of the data is calculated and it was 0.6218°.

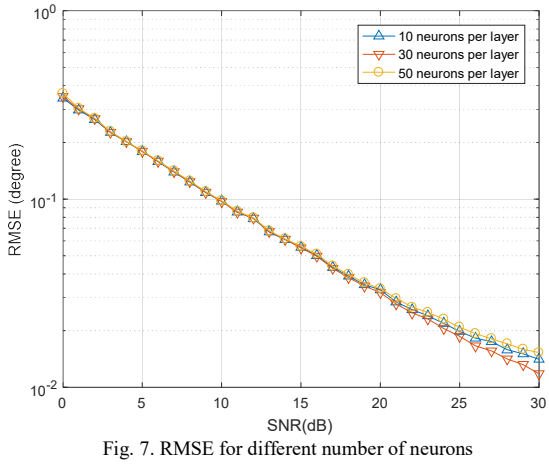

Fig. 7. RMSE for different number of neurons

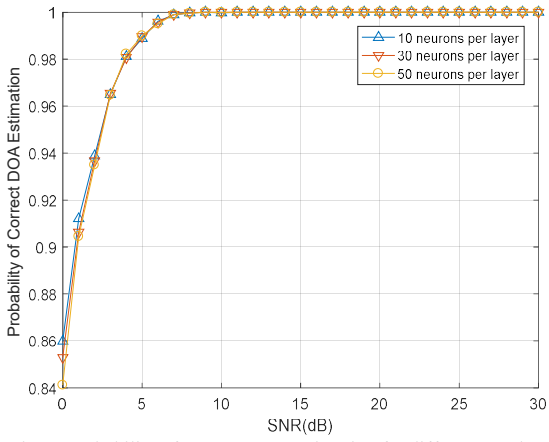

Fig. 8. Probability of correct DOA estimation for different number of neurons

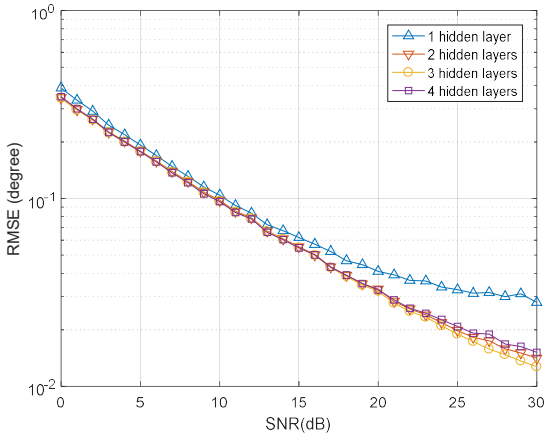

Fig. 9. RMSE for different number of hidden layers

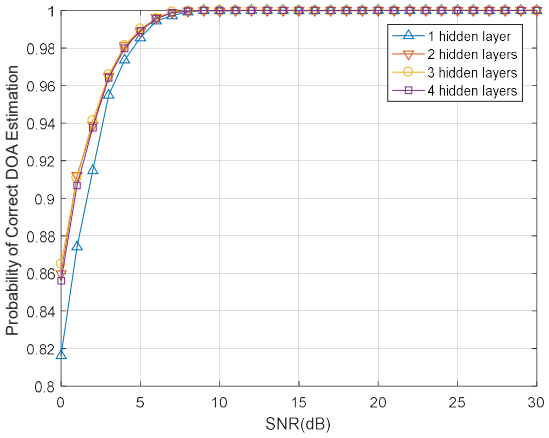

Fig. 10. Probability of correct DOA estimation for different number of hidden layers

IV. Conclusion

In this paper, we simulated a three-level wireless seismic survey model. The wireless seismic survey model was divided to hexagonal cells, and each cell is divided into three sectors. DOA estimation based on deep learning algorithm was considered and the performance of the neural network was investigated by varying three network parameters. The neural network that performed the best was selected to be applied in one sector of the seismic model between geophones and cluster-head nodes, which produced reasonably highly accurate results. In the future, DOA estimation could be utilized for geophone localization, which is essential for interpreting seismic data.

References

[1] J. Caldwell, "Wireless Seismic Systems-""Great Expectations"" T Reduce Seismic Acquisition Cost," in *SEG Technical Program Expanded Abstracts :3834-3837*, 2010.

[2] S. Savazzi and U. Spagnolini, "Wireless geophone networks for high-density land acquisition: Technologies and future potential," *The Leading Edge,* vol. 27, no. 7, pp. 882-886, 2008.

[3] S. Savazzi, U. Spagnolini, L. Goratti, D. Molteni, M. Latva-aho and M. Nicoli, "Ultra-Wide Band Sensor Networks in Oil and Gas Explorations," *IEEE Communications Magazine (Volume: 51 , Issue: 4 , April 2013),* pp. 150 - 160, 11 April 2013.

[4] J. Tian, M. Gao and H. Zhou, "Multi-channel Seismic Data Synchronizing Acquisition System Based on Wireless Sensor Network," in *2008 IEEE International Conference on Networking, Sensing and Control* , Sanya, China, 2008.

[5] S. Savazzi and U. Spagnolin, "Synchronous Ultra-Wide Band Wireless Sensors Networks for oil and gas exploration," in *2009 IEEE Symposium on Computers and Communications*, Sousse, Tunisia, 2009.

[6] S. Savazzi, L. Goratti, D. Fontanella, M. Nicoli and U. Spagnolini, "Pervasive UWB sensor networks for oil exploration," in *2011 IEEE International Conference on Ultra-Wideband (ICUWB)*, Bologna, Italy, 2011.

[7] V. A. Reddy, G. L. Stueber and S. I. Al-Dharrab, "Energy Efficient Network Architecture for Seismic Data Acquisition via Wireless Geophones," in *2018 IEEE International Conference on Communications (ICC)*, Kansas City, MO, USA, 2018.

[8] S. Alawsh, A. Muqaibel and M. Sharawi, "DOA estimation in MIMO systems with Compressive Sensing for future handsets," in *2015 IEEE Jordan Conference on Applied Electrical Engineering and Computing Technologies (AEECT)*, Amman, Jordan, 2015.

[9] S. Abeywickrama, L. Jayasinghe, H. Fu, S. Nissanka and C. Yuen, "RF-based direction finding of UAVs using DNN," in *IEEE International Conference on Communication Systems (ICCS) 2018*, 2018.

[10] Y. Kase, T. Nishimura, T. Ohgane, Y. Ogawa, D. Kitayama and Y. Kishiyama, "DOA Estimation of Two Targets with Deep Learning," in *2018 15th Workshop on Positioning, Navigation and Communications (WPNC)*, Bremen, Germany, 2018.

[11] Z. Liu, C. Zhang and Y. P. S, "Direction-of-Arrival Estimation Based on Deep Neural Networks With Robustness to Array Imperfections," *IEEE Transactions on Antennas and Propagation,* vol. 66, no. 12 , Dec. 2018, pp. 7315-7327, 2018.

[12] L.-l. Wu, Z.-m. Liu and H. Zhi-tao, "Deep Convolution Network for Direction of Arrival Estimation with Sparse Prior," *IEEE Signal Processing Letter ,* pp. 1-1, 2019.

[13] H. Huang, J. Yang, H. Huang, Y. Song and G. Gui, "Deep Learning for Super-Resolution Channel Estimation and DOA Estimation Based Massive MIMO System," *IEEE Transactions on Vehicular Technology,* vol. 67 , no. 9, pp. 8549 - 8560, 2018.

[14] M. F. Ünlerşen and E. Yaldiz, "Direction of Arrival Estimation by Using Artificial Neural Networks," in *European Modelling Symposium (EMS)*, Pisa, Italy, 2016.